PLEASE CITE THIS ARTICLE AS DOI: 10.1063/5.0098336

Quadratic pseudospectrum for identifying localized states Alexander Cerjan* Center for Integrated Nanotechnologies

Alexander Cerjan*

Center for Integrated Nanotechnologies

Sandia National Laboratories

Albuquerque, New Mexico 87185, USA

Terry A. Loring[†]

Department of Mathematics and Statistics

University of New Mexico

Albuquerque, New Mexico, 87123, USA

Fredy Vides[‡]

Scientific Computing Innovation Center School of Mathematics and Computer Science Universidad Nacional Autónoma de Honduras Tegucigalpa, Honduras (Dated: January 3, 2023)

We examine the utility of the quadratic pseudospectrum for understanding and detecting states that are somewhat localized in position and energy, in particular in the context of condensed matter physics. Specifically, the quadratic pseudospectrum represents a method for approaching systems with incompatible observables $\{A_j \mid 1 \leq j \leq d\}$, as it minimizes collectively the errors $\|A_j v - \lambda_j v\|$ while defining a joint approximate spectrum of incompatible observables. Moreover, we derive an important estimate relating the Clifford and quadratic pseudospectra. Finally, we prove that the quadratic pseudospectrum is local, and derive the bounds on the errors that are incurred by truncating the system in the vicinity of where the pseudospectrum is being calculated.

^{*} awcerja@sandia.gov

 $^{^{\}dagger}$ loring@math.unm.edu

[‡] fredy.vides@unah.edu.hn

PLEASE CITE THIS ARTICLE AS DOI: 10.1063/5.0098336

I. INTRODUCTION

Many fields in modern physics are faced with the challenge of trying to glean information from incompatible observables in a system. Although this problem is most closely associated with the Heisenberg uncertainty principle in quantum mechanics, it also commonly manifests in classical systems governed by a wave equation. As an example, consider a point defect in a crystalline lattice that can host localized states [19]. For such a system, the most important questions are: (1) what are the energies of the defect states, and (2) what are their spatial extents. Unfortunately, these questions correspond to incompatible observables, as in general the Hamiltonian for a crystal, H, does not commute with the crystal's position operators, X_j with $j=1,2,3, [H,X_j] \neq 0$. Typically, this problem is approached by first finding the spectrum of H over some suitably large volume containing a single defect to find the energies of the defect's states. If the energy of a defect state, $|\psi_{\text{def}}\rangle$, is in a bulk band gap of the surrounding crystal, a measure of the location and localization of this state can then be determined using moments of the state's position expectation values, $\langle \psi_{\rm def} | X_i^n | \psi_{\rm def} \rangle$. However, when a defect state's energy is within the extent of the crystal's bulk bands, this approach is no longer possible as any eigenstate of the Hamiltonian associated with the defect is now a member of a large degenerate subspace. While one can always choose an ortho-normal basis for this subspace $\{|\psi_{\rm def}\rangle, |\psi_m\rangle\}$ and associate one of the basis states with the defect (m indexes the other chosen basis states), it is always possible to construct $|\psi'_{\text{def}}\rangle = (1/N)(|\psi_{\text{def}}\rangle + \sum_{m} a_m |\psi_m\rangle)$, which is an equally valid eigenstate of H. Here, N is a normalization constant and a_m are modal coefficients. Moreover, generically, $\langle \psi_{\mathrm{def}} | X_{j}^{n} | \psi_{\mathrm{def}} \rangle \neq \langle \psi_{\mathrm{def}}' | X_{j}^{n} | \psi_{\mathrm{def}}' \rangle$, i.e., different choices of the defect's eigenstate will yield different position expectation values. Thus, when the defect state becomes degenerate with the surrounding bulk crystal modes, more sophisticated techniques are required to determine its localization.

One approach for finding an approximate joint eigenspectrum between non-commuting operators is to study the system using pseudospectral methods that do not require directly measuring any of the system's incompatible observables individually. Intuitively, this approach is based on constructing a single composite operator out of the various eigenvalue problems, $(A_j - \lambda_j)v$, for each of the relevant non-commuting operators, A_j , and then analyzing the spectrum (or related aspects) of this composite operator. One example of such a composite operator is the spectral localizer [29],

$$L_{\lambda}(A_1, \dots, A_d) = \sum_{j=1}^d (A_j - \lambda_j) \otimes \Gamma_j, \tag{I.1}$$

which combines the underlying eigenvalue equations using a non-trivial Clifford representation, $\Gamma_j^{\dagger} = \Gamma_j$, $\Gamma_j^2 = I$, and $\Gamma_j \Gamma_l = -\Gamma_l \Gamma_j$ for $j \neq l$. Here, we assume that A_j are Hermitian, so that $\lambda_j \in \mathbb{R}$ and thus

$$\lambda = (\lambda_1, \cdots, \lambda_d) \in \mathbb{R}^d$$
.

We want to know if $L_{\lambda}(A_1, \dots, A_d)$ is singular, and if not, how far it deviates from singular. No matter how close the localizer is to being singular, its spectrum can contain valuable information on a material's topological properties [29], including the number of Dirac or Weyl points in its spectrum at a given energy [46] or on the manner in which edge modes propagate in the presence of strong disorder [39]. Note that there has been a subtle shift in the treatment of λ_j in Eq. (I.1) as compared to its use in an eigenvalue equation. Whereas in an eigenvalue problem, $(A_j - \lambda_j)v = 0$, λ_j is something that is calculated using a known operator (i.e., λ_j is a dependent variable), in a composite operator λ is better thought of as an input (i.e., as a set of independent variables).

Even when there is no topology to study, the utility of composite operators is providing for incompatible observables some metric for the inherent uncertainty in joint measurement given a state whose expectation in these observables is close to λ . For example, at a given λ the localizer can be used to define the *localizer gap* of (A_1, \dots, A_d) as

$$\mu_{\lambda}^{C}(A_1, \dots, A_d) = \sigma_{\min}(L_{\lambda}(A_1, \dots, A_d)).$$

Here we use $\sigma_{\min}(M)$ to denote the smallest singular value of M. (Mainly we use this in the case where M is Hermitian and so $\sigma_{\min}(M)$ is the smallest absolute value of an eigenvalue.) Finally, the localizer can be used to define the *Clifford* ϵ -pseudospectrum [29, §1],

$$\Lambda_{\epsilon}^{C}(A_{1},\cdots,A_{d})=\{\boldsymbol{\lambda}\mid \mu_{\boldsymbol{\lambda}}^{C}(A_{1},\cdots,A_{d})\leq \epsilon\}$$

which is a closed subset of \mathbb{R}^d . When $\epsilon = 0$ this set is known simply as the Clifford spectrum. Those λ that yield small localizer gaps correspond to joint approximate eigenvalues of (A_1, \dots, A_d) . Thus, the utility of composite operators and pseudospectral methods can be understood as enabling the simultaneous, but approximate, joint measurement of many



PLEASE CITE THIS ARTICLE AS DOI: 10.1063/5.0098336

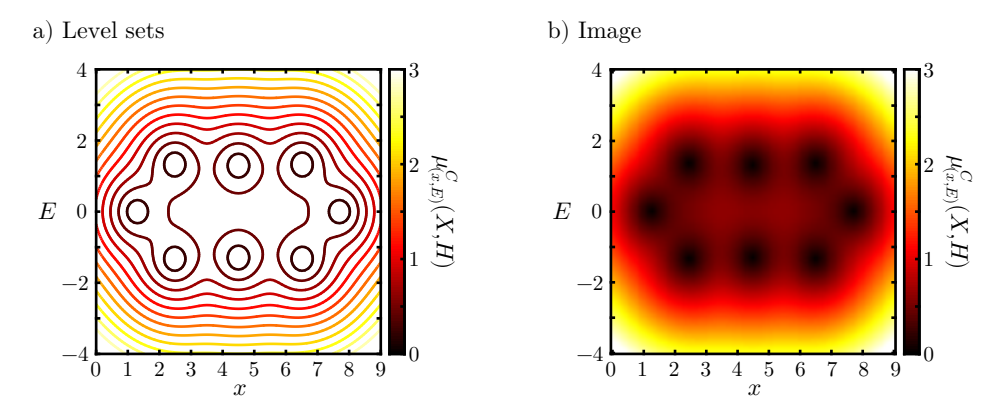


FIG. 1. The Clifford pseudospectrum associated to the two observables defining a basic SSH model. This is shown as the traditional level sets and as an image with artificial color. The value of the indicator function hits zero at eight points, two of which correspond to defect states at zero energy.

incompatible observables. Note though, that even if λ is a member of the Clifford spectrum of (A_1, \dots, A_d) , it does not follow that λ_j is necessarily an eigenvalue of A_j .

There is a direct connection of traditional pseudospectrum [50, 51] with the Clifford pseudospectrum of two Hermitian matrices. For a general square matrix N, its ϵ -pseudospectrum is the set

$$\{z \in \mathbb{C} \mid \|(N-z)^{-1}\|^{-1} \le \epsilon\}$$

with the convention that $||Y^{-1}||^{-1} = 0$ in the singular case. Again this is the spectral norm and so it is equivalent to say the ϵ -pseudospectrum of N is the set of complex numbers where $\sigma_{\min}(N-z)$ is less than ϵ . If $N = A_1 + iA_2$ for Hermitian matrices A_1 and A_2 , then the singular values of $N - (\lambda_1 + i\lambda_2)$ equal the eigenvalues of

$$\begin{bmatrix} 0 & N^\dagger - (\lambda_1 - i\lambda_2) \\ N - (\lambda_1 + i\lambda_2) & 0 \end{bmatrix} = \begin{bmatrix} 0 & (A_1 + iA_2)^\dagger - (\lambda_1 - i\lambda_2) \\ (A_1 + iA_2) - (\lambda_1 + i\lambda_2) & 0 \end{bmatrix} = L_{(\lambda_1 + i\lambda_2)}(A_1, A_2)$$

we see that the ϵ -pseudospectrum of N becomes the Clifford ϵ -pseudospectrum of (A_1, A_2) once we identify \mathbb{C} with \mathbb{R}^2 . Traditionally, pseudospectra are displayed by curves indicating the boundaries of several different ϵ -pseudospectra. These are the level curves of the function

$$\lambda \mapsto \mu_{\lambda}^{C}(A_1, \cdots, A_d).$$

We refer to this as the *indicator function* for the Clifford pseudospectrum. We prefer to display the indicator function as an image as this is closer to how most synthetic and experimental data are presented in physics. In Figure 1 we illustrate the two-variable Clifford pseudospectrum for (X, H), the Hamiltonian and position observable for a standard finite Su-Schrieffer-Heeger (SSH) model [49] (see, for example, [2, §1.1])

with v = 0.7 and w = 1.4. This will have a defect state at each end reflecting its non-trivial K-theory.

Previously, the Clifford pseudospectrum has attracted interest due to its close connection with a system's K-theory [32, 33], which can be used to diagnose a material's topological properties [3, 14, 20, 41, 55]. When the H_j are H and X_i for a crystal, the localizer can be used to determine the crystal's topology in all (physical) dimensions and every symmetry class, regardless of whether the system exhibits a bulk bandgap [10]. Moreover, changes in the system's topology can only occur when the localizer gap closes, i.e., at λ where $\mu_{\lambda}^{C}(A_1, \dots, A_d) = 0$. However, despite these

PLEASE CITE THIS ARTICLE AS DOI: 10.1063/5.0098336

This is the author's peer reviewed, accepted manuscript. However, the online version of record will be different from this version once it has been copyedited and typeset

beneficial properties of the localizer, its structure necessarily increases the computational complexity of solving for the system's approximate spectrum beyond the complexity of finding the Hamiltonian's exact spectrum due to the need to tensor the constituent operators with a Clifford representation. (This can be especially problematic in 3D systems where an n-by-n-by-n system's localizer has size at least $4n^3$ -by- $4n^3$.) The increased computational complexity of the localizer presents two related questions: (1) Given that a wide range of physical systems do not possess non-trivial topology, is there a composite operator which can be used to efficiently solve for approximate joint spectra? (2) Even for systems that exhibit topological behaviors where the localizer might be necessary, can we estimate the size of the localizer gap using the pseudospectrum of a composite operator with the same size as the system's Hamiltonian?

Here, we establish the physical relevance of the quadratic composite operator,

$$Q_{\lambda}(A_1,\cdots,A_d) = \sum_{j=1}^d (A_j - \lambda_j)^2,$$

which can be used to calculate what is called the quadratic pseudospectrum [34]. The quadratic pseudospectrum is a collection of sets determined by an indicator function, defined below. The value of this indicator function at λ tells us about how small the variances in all the observables can be for a state centered at λ . By centered, we mean $|\psi\rangle$ has expectation value λ_j in the jth observable. The value of the indicator function can be computed in terms of an eigenvalue of Q_{λ} . Moreover, we provide a bound on the maximum difference between the smallest singular values of the quadratic composite operator and the localizer. Finally, we prove a number of results that shows the quadratic pseudospectrum is well-behaved in a number of ways that will enable the development of efficient algorithms for its calculation.

The remainder of this paper is organized as follows. In Sec. II we provide some basic definitions and results for the quadratic pseudospectrum. In particular, we establish the upper bound between the quadratic and Clifford pseudospectra, proving that at λ with sufficiently large quadratic gaps, the localizer gap cannot be zero. In Sec. III we prove results regarding the error induced by truncating the spacial extent of a physical system. In Sec. IV we provide some simple examples using small matrices of the behavior of the quadratic and Clifford pseudospectra. In Sec. V we explain why we cannot ignore the Clifford pseudospectrum, namely that the localizer contains K-theory while the quadratic composite operator does not. In Sec. VI we provide some more physically motivated examples of the behavior of both pseudospectra in physical systems with non-trivial topology. Finally, in Sec. VII we offer some concluding remarks.

II. PROPERTIES OF THE QUADRATIC PSEUDOSPECTRUM

We recall that a unit vector v in Hilbert space determines a probability distribution with respect to a Hermitian matrix (observable) X. We do not need access to the full distribution, but only its expectation and variance. This will be enough for us to talk in fuzzy terms about the location of a state or its approximate energy. In mathematical notation, the expectation is

$$E_{\boldsymbol{v}}[A] = \langle A\boldsymbol{v}, \boldsymbol{v} \rangle,$$

and the square of the variance is

$$\Delta_{\mathbf{v}}^2 A = \langle A^2 \mathbf{v}, \mathbf{v} \rangle - \langle A \mathbf{v}, \mathbf{v} \rangle^2.$$

A more typical expression for these quantities in many fields of physics, using $v = |\psi\rangle$, would be

$$\langle A \rangle_{\psi} = \langle \psi | A | \psi \rangle,$$

and

$$\Delta_{\psi}^2 A = \langle \psi | A^2 | \psi \rangle - \langle \psi | A | \psi \rangle^2.$$

If we cannot find an eigenvector and eigenvalue, we can try instead to make $||Av - \lambda v||$ as small as possible. This "eigen-error" occurs naturally in mathematics so long as v is a unit vector. Assuming as well that λ is real, we compute

$$\|A\boldsymbol{v} - \lambda \boldsymbol{v}\|^2 = \langle A^2 \boldsymbol{v}, \boldsymbol{v} \rangle - 2\lambda \langle A\boldsymbol{v}, \boldsymbol{v} \rangle + \lambda^2 = (\langle A^2 \boldsymbol{v}, \boldsymbol{v} \rangle - \langle A\boldsymbol{v}, \boldsymbol{v} \rangle^2) + (\langle A\boldsymbol{v}, \boldsymbol{v} \rangle - \lambda)^2$$

we are able to rewrite this expression as

$$||A\boldsymbol{v} - \lambda \boldsymbol{v}||^2 = \Delta_{\boldsymbol{v}}^2 A + (\mathbf{E}_{\boldsymbol{v}}[A] - \lambda)^2$$
(II.1)

This is the author's peer reviewed, accepted manuscript. However, the online version of record will be different from this version once it has been copyedited and typeset

PLEASE CITE THIS ARTICLE AS DOI: 10.1063/5.009833(

which is the square sum of the variance and the displacement of the expectation from what we were expecting.

As in general $[A_j, A_l] \neq 0$, it is impossible to find exact joint eigenvectors of these operators. The quadratic pseudospectrum instead provides a measurement of how close we can get to a joint eigenvector. The following is built on the ideas in [44, §6]. This theorem relates physically relevant features of states to matrix computations that allow for reasonably fast numerical algorithms.

Proposition II.1. Suppose A_1, \ldots, A_d are n-by-n Hermitian matrices and that λ is an element of \mathbb{R}^d . The following quantities are always equal:

1. the minimum of

$$\sqrt{\sum_{j=1}^{d} \left\| A_j oldsymbol{v} - \lambda_j oldsymbol{v}
ight\|^2}$$

as \mathbf{v} ranges over all unit vectors in \mathbb{C}^n ,

2. the minimum of

$$\sqrt{\sum_{j=1}^{d} \Delta_{\boldsymbol{v}}^{2} A_{j} + \sum_{j=1}^{d} \left(E_{\boldsymbol{v}}[A_{j}] - \lambda_{j} \right)^{2}}$$

as v ranges over all unit vectors in \mathbb{C}^n ,

3. the smallest singular value of

$$M_{\lambda}(A_1, \dots, A_d) = \begin{bmatrix} A_1 - \lambda_1 \\ A_2 - \lambda_2 \\ \vdots \\ A_d - \lambda_d \end{bmatrix},$$
 (II.2)

4. the square root of the smallest eigenvalue of $Q_{\lambda}(A_1, \dots, A_d)$.

Moreover, a unit vector is a right singular vector of (II.2), iff it is an eigenvector of $Q_{\lambda}(A_1, \dots, A_d)$, iff it minimizes the quantity in (1), iff it minimizes the quantity in (2).

Proof. The equality of (1) and (2) follows from (II.1). The equality of (3) and (4) follows from

$$(M_{\lambda}(A_1,\cdots,A_d))^{\dagger}M_{\lambda}(A_1,\cdots,A_d)=Q_{\lambda}(A_1,\cdots,A_d)$$

and the fact that $\sigma_{\min}(B^{\dagger}B) = (\sigma_{\min}(B))^2$ for any matrix B. The final part of the argument uses a characterisation of the smallest singular value of a matrix B (see [17, Thm. 8.6.1]) as

$$\sigma_{\min}(B) = \min_{\|\boldsymbol{v}\|=1} \|B\boldsymbol{v}\|$$

and the routine calculation

$$||M_{\lambda}(A_1,\cdots,A_d)\boldsymbol{v}|| = \sqrt{\sum ||A_j\boldsymbol{v}-\lambda_j\boldsymbol{v}||^2}.$$

Definition II.2. Suppose A_1, \ldots, A_d are Hermitian matrices in $M_n(\mathbb{C})$. For every $\lambda = (\lambda_1, \ldots, \lambda_d)$ in \mathbb{R}^d we define the quadratic gap of (A_1, \ldots, A_d) at λ as

$$\mu_{\lambda}^{Q}(A_1,\ldots,A_d) = (\sigma_{\min}(Q_{\lambda}(A_1,\cdots,A_d)))^{\frac{1}{2}}.$$

The quadratic ϵ -pseudospectrum of (A_1, \ldots, A_d) is defined as the set

$$\Lambda_{\varepsilon}^{Q}(A_{1},\cdots,A_{d})=\{\boldsymbol{\lambda}\mid \mu_{\boldsymbol{\lambda}}^{Q}(A_{1},\cdots,A_{d})\leq \varepsilon\}.$$

When $\epsilon = 0$ this set is known simply as the quadratic spectrum. We call the function

$$\lambda \mapsto \mu_{\lambda}^{Q}(A_1, \ldots, A_d)$$

the indicator function of the quadratic pseudospectrum.

PLEASE CITE THIS ARTICLE AS DOI: 10.1063/5.0098336



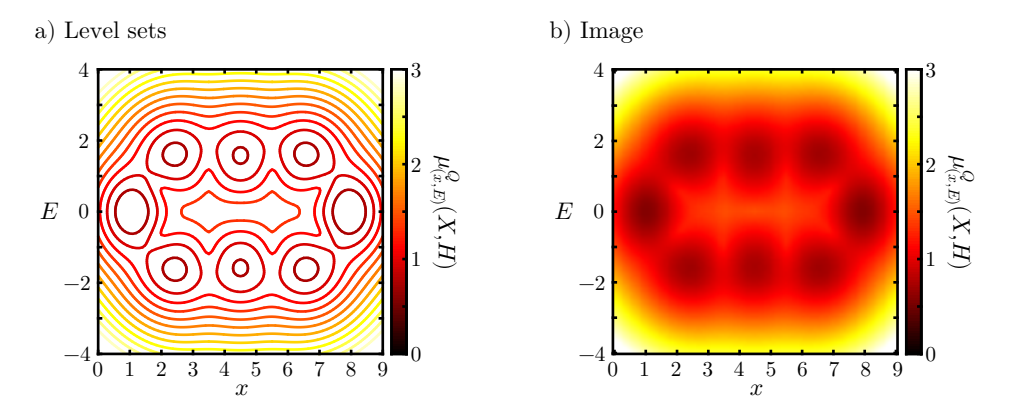


FIG. 2. The quadratic pseudospectrum associated to the two observables defining a basic SSH model. This is shown as the traditional level sets and as an image with artificial color. The value of the indicator function is never zero.

The history of the quadradic pseudospectrum is murky. We suspect that many have considered this construction and quickly rejected it when discovering that the quadratic spectrum of a pair of Hermitian operators is very often empty. Indeed, the middle author has been so rash [15]. The dissertation [57] comes very close to defining the quadratic pseudospectrum [57, §5.3]. The operator $Q_{\lambda}(A_1, \dots, A_d)$ is seen there and in early work [44] on the emergent geometry of D-branes, where it is one possible Hamiltonian for combined system of a probe and a D-brane. An examination of the proofs in [29] will reveal that the quadratic pseudospectrum has been around but not emphasized. When looking at joint approximate eigenvalues, as in [34] or [29] there are efficient algorithms based on the quadratic pseudospectrum for finding joint approximate eigenvalues. On the other hand, it is very hard to calculate examples of the quadratic pseudospectrum when working by hand. This difficulty in examining examples is probably also a contributing factor in this subject not being explored much earlier.

Some basic results about eigenvectors can be tweaked to work with approximate eigenvectors. The following lemma is an example, a modification of the usual fact that for Hermitian matrices, different eigenspaces are orthogonal. Notice there is no sensible interpretation of a subspace of approximate eigenvectors for a fixed scalar. We omit the proof as it is an easy modification of a standard short proof.

Lemma II.3. Suppose that A is a Hermitian matrix and that v and w are unit vectors and $\lambda \neq \mu$ are two real numbers.

$$|\langle \boldsymbol{v}, \boldsymbol{w} \rangle| \leq rac{\|A \boldsymbol{v} - \lambda \boldsymbol{v}\| + \|A \boldsymbol{w} - \mu \boldsymbol{w}\|}{|\lambda - \mu|}.$$

A strange thing is that the quadratic spectrum of (A_1, \ldots, A_d) is often the empty set. One example of this is worked out in [15]. We find another example now by working out the quadratic pseudospectrum for the matrices from (I.2), as illustrated in Figure 2.

We are most interested in the places where the quadratic spectrum is close to or at a local minimum value even if that minimum is not zero. Working with Q_{λ} we can compute examples of a unit vector v so that

$$\sum_{j=1}^{d} \Delta_{\boldsymbol{v}}^2 A_j + \sum_{j=1}^{d} \left(\mathbb{E}_{\boldsymbol{v}} [A_j] - \lambda_j \right)^2$$

is as small as possible. Notice that several lower bounds on the sum of uncertainty have been proven recently [13, 35]. but the proofs of those results do not indicate how to find unit vectors that cause the sum of uncertainty to be small.

There are instances where one should compute both the Clifford and the quadratic pseudospectra to better understand a system. Here the relevant observables are generally the Hamiltonian and all the coordinates of position. This is especially true in studying systems such as topological metals where only the quadratic pseudospectrum can distinguish bound states from bulk states. As it is only the Clifford pseudospectrum that sees the K-theory, we need to understand that as well. Our generic argument for the stability of a bound state is as follows. Places where the Clifford gap is large cannot be closed easily by disorder. If a local invariant changes value between two such places, then even after adding some disorder there will be a location μ between them were $\mu_{\mu}^{C}=0$. The next result shows us $\mu_{\lambda}^{C}\approx\mu_{\lambda}^{Q}$ for all λ and so $\mu_{\mu}^{Q}\approx0$ and there must be a state rather localized around μ , so localized in energy and position. For a topological insulator with no

This is the author's peer reviewed, accepted manuscript. However, the online version of record will be different from this version once it has been copyedited and typeset

PLEASE CITE THIS ARTICLE AS DOI: 10.1063/5.0098336

disorder, as in Figure 7, there is really no need to calculate too much beyond parts of the Clifford pseudospectrum. If a system has heavy disorder, or is a topological metal as in Figure 10, where we extend a little the analysis from [10], a full analysis will require looking at the Clifford and the quadratic pseudospectra and probably also the local density of states.

Proposition II.4. If A_1, \ldots, A_d are Hermitian matrices in $\mathbf{M}_n(\mathbb{C})$ and $\lambda \in \mathbb{R}^d$ then

$$\left| \left(\mu_{\lambda}^{Q}(A_1, \dots, A_d) \right)^2 - \left(\mu_{\lambda}^{C}(A_1, \dots, A_d) \right)^2 \right| \le \sum_{j \le k} \| [A_j, A_k] \|. \tag{II.3}$$

Proof. Since tensoring by the identity will not alter the spectrum of a matrix,

$$\sigma_{\min}\left(\sum (A_j - \lambda_j)^2\right) = \sigma_{\min}\left(\sum (A_j - \lambda_j)^2 \otimes I\right).$$

We also have the estimate

$$(L_{\lambda}(A_1, \dots, A_d))^2 = \sum (A_j - \lambda_j)^2 \otimes I + \sum_{j \le k} [A_j, A_k] \otimes \Gamma_j \Gamma_k$$
 (II.4)

and so

$$\|(L_{\lambda}(A_1, \dots, A_d))^2 - \sum (A_j - \lambda_j)^2 \otimes I\| \leq \sum_{j < k} \|[A_j, A_k]\|.$$

We can again use the Lipschitz continuity of the smallest singular value and we find that

$$\left| \sigma_{\min} \left(L_{\lambda}(A_1, \cdots, A_d) \right)^2 - \sigma_{\min} \left(\sum (A_j - \lambda_j)^2 \otimes I \right) \right| \leq \sum_{j \leq k} \left\| [A_j, A_k] \right\|.$$

A difficulty in determining either pseudospectra of a noncommutative d-tuple is that calculating the value at one or more values of λ does not provide much assistance in calculating the value at another value. We do, at least, have a sense of how fast μ_{λ}^{C} or μ_{λ}^{Q} can vary, so can limit the number of values of λ that need to be considered. We know from results in [29, §7] that μ_{λ}^{C} is Lipschitz with constant 1. We next show that the same is true in the quadratic case.

Proposition II.5. Suppose A_1, \ldots, A_d are Hermitian matrices in $M_n(\mathbb{C})$. If λ, μ are two elements of \mathbb{R}^d then

$$\left|\mu_{\lambda}^{Q}(A_{1},\ldots,A_{d})-\mu_{\nu}^{Q}(A_{1},\ldots,A_{d})\right|\leq\|\lambda-\nu\|$$

where the norm on the right is the Euclidean norm.

Proof. It is well known that all singular values are Lipshitz in the matrix input A, so long as one uses the operator norm to give the metric on the space of m-by-n matrices. For example, one can apply Weyl's inequality to the eigenvalues of the Hermitian matrix

$$\left[\begin{array}{cc} 0 & A \\ A^{\dagger} & 0 \end{array}\right].$$

Finally,

$$\|M_{\lambda}(A_1, \dots, A_d) - M_{\mu}(A_1, \dots, A_d)\|^2 = \left\| \begin{bmatrix} (\lambda_1 - \mu_1)I \\ \vdots \\ (\lambda_d - \mu_d)I \end{bmatrix} \right\|^2$$

$$= \left\| \begin{bmatrix} (\lambda_1 - \mu_1)I & \cdots & (\lambda_d - \mu_d)I \end{bmatrix} \begin{bmatrix} (\lambda_1 - \mu_1)I \\ \vdots \\ (\lambda_d - \mu_d)I \end{bmatrix} \right\|$$

$$= \left\| \left(\sum (\lambda_1 - \mu_1)^2 \right) I \right\|$$

$$= \sum (\lambda_1 - \mu_1)^2.$$

PLEASE CITE THIS ARTICLE AS DOI: 10.1063/5.0098336

III. THE LOCAL NATURE OF THE QUADRATIC PSEUDOSPECTRUM

As the quadratic pseudospectrum should be relatively easier to compute numerically than its sibling, the Clifford pseudospectrum, we want as many shortcuts and optimizations as possible for computing it. In [30] it was shown that truncating a system spatially had little effect on the Clifford pseudospectrum, so long as the truncation happened well away from the probe-point (x, y). Here we establish a similar bound on the effect spacial truncation can have on the quadratic pseudospectrum.

We will assume only that the first d Hermitian matrices commute with each other. We call these X_j to suggest these are position observables, but that is not important. The last Hermitian matrix we call H.

For simplicity, we will assume always $\lambda = 0$. We can form the Hermitian matrix

$$Z = \sqrt{X_1^2 + \cdots X_d^2}$$

which we can think of as Euclidean distance from the origin in the spacial coordinates. In what follows, we make the simplifying assumption that Z is invertible. This just means that our model cannot have a site located at exactly the origin. Since the quadratic pseudospectrum is Lipschitz in position we can easily work around this, if needed, to get estimates that work without this assumption.

We deal with truncation in two steps. First we contemplate what can happen to the quadratic pseudospectrum at $\mathbf{0}$ if we alter how H acts on parts of the Hilbert space far away from the origin. In particular, if we set H to act as zero out there using some physical assumption of locality in the system being described. The second step is to deal with the effect of excising that part of the Hilbert space where H is now acting trivially.

The first part is in the following Theorem. This will have applications beyond truncation, as it tells us that the quadratic pseudospectrum is generally unaffected by defects far away from the the "probe" location.

Theorem III.1. Assume X_1, \ldots, X_d and H are Hermitian matrices of the same size, that the X_j commute with each other, and that

$$Z = \sqrt{X_1^2 + \cdots X_d^2}$$

is invertible. If H_0 is Hermitian and

$$||Z^{-1}(HH_0 + HH_0 + H_0^2)Z^{-1}|| \le C$$
 (III.1)

for some constant C with C < 1, then

$$(1-C)^{\frac{1}{2}}\mu_{\mathbf{0}}^{Q}(X_{1},\ldots,X_{d},H) \leq \mu_{\mathbf{0}}^{Q}(X_{1},\ldots,X_{d},H+H_{0}) \leq (1+C)^{\frac{1}{2}}\mu_{\mathbf{0}}^{Q}(X_{1},\ldots,X_{d},H).$$

Proof. With the above definition of Z we obtain

$$Q_0(X_1,\ldots,X_d,H) = Z^2 + H^2$$

and

$$Q_0(X_1, \dots, X_d, H + H_0) = Z^2 + H^2 + HH_0 + H_0H + H_0^2.$$

Multiplying (III.1) by Z on both sides leads to

$$-CZ^{2} \le HH_{0} + HH_{0} + H_{0}^{2} \le CZ^{2}. \tag{III.2}$$

Thus

$$Q_0(X_1, \dots, X_d, H + H_0) \le Z^2 + H^2 + C|Z|^2$$

$$\le (1+C)(Z^2 + H^2)$$

$$= (1+C)Q_0(X_1, \dots, X_d, H)$$

and

$$Q_{\mathbf{0}}(X_1, \dots, X_d, H + H_0) \ge Z^2 + H^2 - C|Z|^2$$

$$\ge (1 - C)(Z^2 + H^2)$$

$$= (1 - C)Q_{\mathbf{0}}(X_1, \dots, X_d, H)$$

This is the author's peer reviewed, accepted manuscript. However, the online version of record will be different from this version once it has been copyedited and typeset.

PLEASE CITE THIS ARTICLE AS DOI: 10.1063/5.0098336

so

$$(1-C)Q_0(X_1,\ldots,X_d,H) \le Q_0(X_1,\ldots,X_d,H+H_0) \le (1+C)Q_0(X_1,\ldots,X_d,H).$$

Thus we have

$$(1+C)^{-1} (Q_0(X_1,\ldots,X_d,H))^{-1} \le Q_0(X_1,\ldots,X_d,H+H_0)^{-1} \le (1-C)^{-1} (Q_0(X_1,\ldots,X_d,H))^{-1}.$$

This means

$$(1+C)^{-1} \left\| (Q_{\mathbf{0}}(X_1, \dots, X_d, H))^{-1} \right\| \le \left\| Q_{\mathbf{0}}(X_1, \dots, X_d, H + H_0)^{-1} \right\|$$

$$\le (1-C)^{-1} \left\| (Q_{\mathbf{0}}(X_1, \dots, X_d, H))^{-1} \right\|$$

and finally

$$(1-C)^{\frac{1}{2}} \left\| (Q_{\mathbf{0}}(X_1, \dots, X_d, H))^{-1} \right\|^{-\frac{1}{2}} \le \left\| Q_{\mathbf{0}}(X_1, \dots, X_d, H + H_0)^{-1} \right\|^{-\frac{1}{2}}$$

$$\le (1+C)^{\frac{1}{2}} \left\| (Q_{\mathbf{0}}(X_1, \dots, X_d, H))^{-1} \right\|^{-\frac{1}{2}}.$$

Theorem III.2. Assume X_1, \ldots, X_d are diagonal matrices and H is a Hermitian matrix, all in $\mathbf{M}_n(\mathbb{C})$, and set

$$Z = \sqrt{X_1^2 + \dots X_d^2}.$$

Let \mathcal{H}_{ρ} denote the Hilbert subspace of \mathbb{C}^n corresponding to standard basis vectors where Z takes value at most ρ . Let $X_1^{\rho}, \ldots, X_d^{\rho}$ and H^{ρ} denote the compressions to \mathcal{H}_{ρ} . If H acts trivially on the complement of \mathcal{H}_{ρ} then

$$Q_{\mathbf{0}}(X_1,\ldots,X_d,H) = \min\left(\rho,Q_{\mathbf{0}}(X_1^{\rho},\ldots,X_d^{\rho},H^{\rho})\right).$$

Proof. The difference between

$$\mu_{\mathbf{0}}^{Q}(X_1,\ldots,X_d,H)$$

and

$$\mu_{\mathbf{0}}^{Q}(X_{1}^{\rho},\ldots,X_{d}^{\rho},H^{\rho})$$

is the addition of many small summands of the form

$$\sum_{j=1}^{d} \lambda_j \Gamma_j + 0\Gamma_{d+1}.$$

Each contributes two points to the spectrum, specifically $\pm \left(\sum_{j=1}^{d} \lambda_j\right)^{\frac{1}{2}}$.

The earlier result on the local nature of the Clifford pseudospectrum, Theorem 7.1 in [30], is not as strong as Theorem III.1. That bound contains terms $||[H, X_i]||$ that seem inevitable due to their appearance in Prop. II.4.

IV. MATHEMATICAL EXAMPLES

Recall that the traditional form of the pseudospectrum arose as a way to investigate a single matrix N that is not normal [50]. We can write N in the usual way, in terms of two Hermitian matrices

$$N = X + iY$$

where $X = \frac{1}{2}(N^{\dagger} + N)$ and $Y = \frac{i}{2}(N^{\dagger} - N)$. The quadratic pseudospectrum

$$\mu_{(x,y)}^{Q}(X,Y) = \min_{\|\boldsymbol{v}\|=1} \sqrt{\|X\boldsymbol{v} - x\boldsymbol{v}\|^2 + \|Y\boldsymbol{v} - y\boldsymbol{v}\|^2}$$

looks for good approximate eigenvectors for X and Y at the same time, while the Clifford pseudospectrum

$$\mu_{(x,y)}^C(X,Y) = \min_{\|{\bm v}\|=1} \|N{\bm v} - (x+iy){\bm v}\|$$

looks for exact and approximate eigenvectors of A which might correspond to complex eigenvalues. To see that later claim, notice that if we select σ_x and σ_y as our Γ matrices then

$$L_{(x,y)}(X,Y) = \begin{bmatrix} 0 & X - iY - (x - iy) \\ X + iY - (x + iy) & 0 \end{bmatrix}.$$

Here we use σ_x , σ_y and σ_z to denote the usual 2-by-2 Pauli matrices.

The traditional pseudospectrum of a non-normal matrix has been applied in physics to assist with the analysis of lossy systems [21, 24, 36, 40, 48].

A. A 2-by-2 pair

Here we use the Pauli matrices themselves as our example, so we let

$$X = \left[\begin{array}{cc} 0 & 1 \\ 1 & 0 \end{array} \right]$$

and

This is the author's peer reviewed, accepted manuscript. However, the online version of record will be different from this version once it has been copyedited and typeset

PLEASE CITE THIS ARTICLE AS DOI: 10.1063/5.0098336

$$Y = \left[\begin{array}{cc} 0 & -i \\ i & 0 \end{array} \right].$$

In this example,

$$N = X + iY = \left[\begin{array}{cc} 0 & 2 \\ 0 & 0 \end{array} \right]$$

is nilpotent. Thus the spectrum of A is just $\{0\} \subseteq \mathbb{C}$ and so the Clifford pseudospectrum of (X,Y) has one zero, at $(0,0) \in \mathbb{R}^2$. This is one of the few cases for which we can easily calculate by hand both the Clifford and quadratic pseudospectra.

We need the singular values of

$$N - \lambda = \left[\begin{array}{cc} -\lambda & 2\\ 0 & -\lambda \end{array} \right]$$

(with $\overline{\lambda} = x + iy$) so the square roots of the eigenvalues of

$$\begin{bmatrix} |\lambda|^2 + 4 & -2\overline{\lambda} \\ -2\lambda & |\lambda|^2 \end{bmatrix}.$$

This has characteristic polynomial (in α)

$$\begin{vmatrix} |\lambda|^2 + 4 - \alpha & -2\overline{\lambda} \\ -2\lambda & |\lambda|^2 - \alpha \end{vmatrix} = \alpha^2 + (-2|\lambda|^2 - 4)\alpha + |\lambda|^4$$

PLEASE CITE THIS ARTICLE AS DOI: 10.1063/5.0098336

so the eigenvalues are

$$\frac{-\left(-2|\lambda|^2 - 4\right) \pm \sqrt{\left(-2|\lambda|^2 - 4\right)^2 - 4\left(|\lambda|^4\right)}}{2} = |\lambda|^2 + 2 \pm 2\sqrt{|\lambda|^2 + 1}.$$

We want the square root of the smaller, so we have computed

$$\mu_{(x,y)}^{C}(X,Y) = \sqrt{x^2 + y^2 + 2 - 2\sqrt{x^2 + y^2 + 1}}.$$

As to the quadratic pseudospectrum of (X,Y), we need the square root of the smallest eigenvalue of

$$(X-x)^2 + (Y-y)^2 = \begin{bmatrix} |\lambda|^2 + 2 & -2\overline{\lambda} \\ -2\lambda & |\lambda|^2 + 2 \end{bmatrix}.$$

This has characteristic polynomial

$$\begin{vmatrix} |\lambda|^2 + 2 - \alpha & -2\overline{\lambda} \\ -2\lambda & |\lambda|^2 + 2 - \alpha \end{vmatrix} = \alpha^2 + \left(-2|\lambda|^2 - 4\right)\alpha + |\lambda|^4 + 4|\lambda|^2 + 4$$

so the eigenvalues are

$$\frac{-\left(-2|\lambda|^2 - 4\right) \pm \sqrt{\left(-2|\lambda|^2 - 4\right)^2 - 4\left(|\lambda|^4 + 4|\lambda|^2 + 4\right)}}{2} = |\lambda|^2 + 2 \pm 2|\lambda|.$$

We want the square root of the smaller, so we have computed

$$\mu_{(x,y)}^Q(X,Y) = \sqrt{x^2 + y^2 + 2 - 2\sqrt{x^2 + y^2}}.$$

In this example, the Clifford pseudospectrum has minimum value of 0, attained at the one point (x, y) = (0, 0). In contrast, the quadratic pseudospectrum has minimum value of 1 attained on the unit circle. Notice that at (0, 0) the difference between the squares of the two pseudospectra is 2, equaling the norm of the commutator of A and B. Thus the estimate in Proposition II.4 is the best possible, at least for the case of a pair of matrices.

It is interesting to note that the Clifford spectrum of the three Pauli spin matrices is the unit sphere, while the Clifford spectrum of any two of them is a singleton. This is just one of the nonintuitive features of the Clifford spectrum [15].

B. A 3-by-3 pair

A slightly larger example is the pair

$$X = \left[\begin{array}{ccc} 0 & 1 & 0 \\ 1 & 0 & 1 \\ 0 & 1 & 0 \end{array} \right]$$

and

$$Y = \left[\begin{array}{ccc} 0 & 1 & 0 \\ 1 & 0 & 0 \\ 0 & 0 & 0 \end{array} \right]$$

corresponding to the one non-normal matrix

$$N = X + iY = \begin{bmatrix} 0 & 1+i & 0\\ 1+i & 0 & 1\\ 0 & 1 & 0 \end{bmatrix}.$$

This has eigenvalues at 0 and approximately $\pm (1.272 + 0.786i)$. Figure 3 shows the two pseudospectra for this pair of matrices.

ACCEPTED MANUSCRIPT

This is the author's peer reviewed, accepted manuscript. However, the online version of record will be different from this version once it has been copyedited and typeset

PLEASE CITE THIS ARTICLE AS DOI: 10.1063/5.0098336

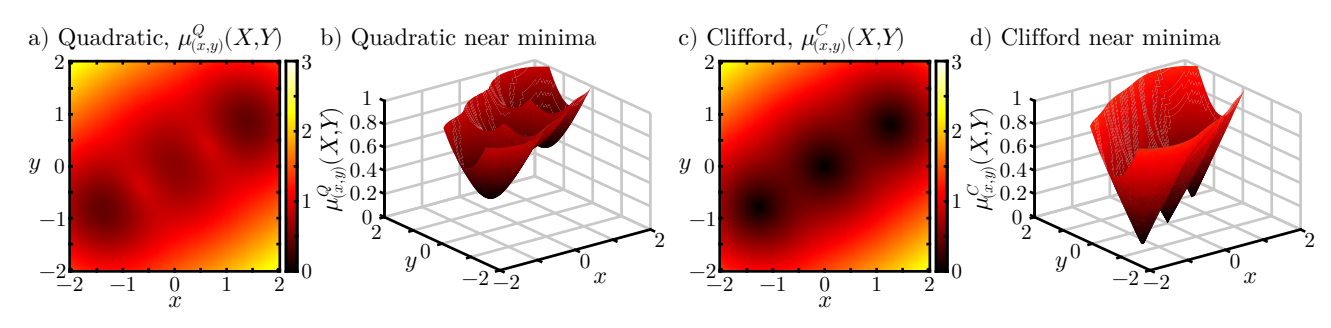


FIG. 3. Both the quadratic and Clifford pseudospectra are shown for the 3-by-3 pair of matrices discussed in Sec. IV B.

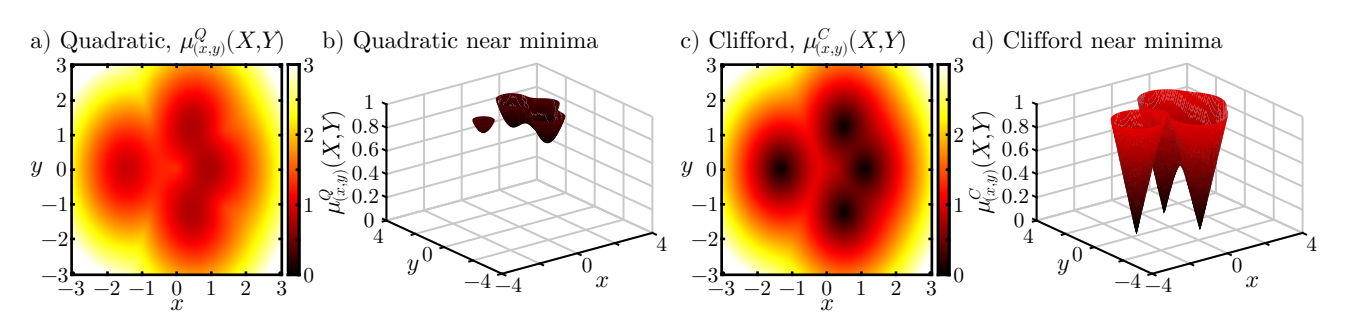


FIG. 4. Both the quadratic and Clifford pseudospectra are shown for the 4-by-4 pair of matrices discussed in Sec. IV C where one of the matrices is real and the other is purely imaginary.

C. A 4-by-4 pair

For a third example we let N = X + iY with

$$X = \begin{bmatrix} -2 & 0 & 0 & 0 \\ 0 & 2 & 0 & 0 \\ 0 & 0 & 0 & 0 \\ 0 & 0 & 0 & 1 \end{bmatrix}$$

and

$$Y = \begin{bmatrix} 0 & i & 0 & 0 \\ -i & 0 & i & 0 \\ 0 & -i & 0 & i \\ 0 & 0 & -i & 0 \end{bmatrix}.$$

Since one of our matrices is real and the other purely imaginary, this is reminiscent of a model of a 1D system in class D [1, 43]. Thus X + iY is real, and there is a \mathbb{Z}_2 topological index related to this example, which is the sign of the determinant of X + iY [29] (see also Section V). In this case, the determinant is negative, which means we can expect one or three eigenvalues on the negative part of the real axis. Figure 4 shows the two pseudospectra for this pair of matrices. The real eigenvalues are approximately -1.7638 and 1.4400 while the complex pair is approximately $0.6619 \pm 1.2371i$.

The quadratic pseudospectrum gives a methodology to attack the problem of finding a unit vector v in \mathbb{R}^n to minimize

$$||X\boldsymbol{v} - x\boldsymbol{v}||^2 + ||Y\boldsymbol{v} - y\boldsymbol{v}||^2$$

given a fixed pair (x, y) of scalars. Many related questions come to mind, such as optimizing by varying both v and (x, y). One can also seek joint approximate eigenvectors v_1, \ldots, v_k for $1 < k \le n$ and perhaps require these vectors to be orthogonal. The case when k = n is the optimization problem addressed by the JADE algorithm [7]. Moreover, when $k \ll n$ it is possible to combine quadratic pseudospectrum method with JADE to get a small number of orthogonal joint approximate eigenvectors [34]. While this may have applications in physics [37] we are content to have this paper focus on the problems related to a single joint approximate eigenvector.

PLEASE CITE THIS ARTICLE AS DOI: 10.1063/5.0098336

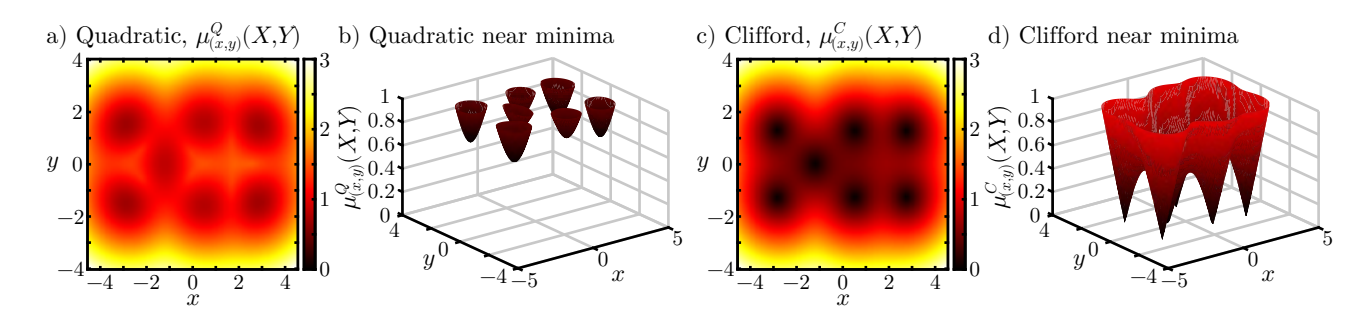


FIG. 5. Both the Clifford and quadratic pseudospectra are shown for two small Hermitian that represent a small system in class D with a defect induced by a phase change.

AB phase change in Class D

A slight variation on the last example is more relevant to topological insulators. In a tight-binding model of a 1D system in symmetry class D we expect a position operator X that is real symmetric (even diagonal) and a Hamiltonian H that is purely imaginary.

In this example we work with

$$X = \begin{bmatrix} -3.5 \\ -2.33 \\ -1.17 \\ 0 \\ 1.17 \\ 2.33 \\ 3.5 \end{bmatrix}$$

and

$$H = \begin{bmatrix} 0 & 1.4i & & & & & \\ -1.4i & 0 & 0.7i & & & & \\ & -0.7i & 0 & 0.7i & & & \\ & & -0.7i & 0 & 1.4i & & \\ & & & & -1.4i & 0 & 0.7i & \\ & & & & & -0.7i & 0 & 1.4i \\ & & & & & -1.4i & 0 \end{bmatrix}.$$

This is reminiscent of an AB phase change in the SSH model. Notice this system has an odd number of sites, in line with previous theory [49] and experiment [38, 53].

The real matrix X + iH has a negative determinant, so it is not surprising that it has a single real eigenvalue and six conjugate pairs of complex eigenvalues. What is remarkable is that the negative eigenvalue is at the location of the AB phase transition, and that it is not easily moved by perturbation.

For the record: The real eigenvalue is approximately -1.1603 while the complex pairs are approximately $-2.7876 \pm$ 1.2941i and $2.8020 \pm 1.2703i$.

Symmetries in the pseudospectra

Many of the previous examples had apparent symmetries in both the Clifford and Quadratic pseudospectra, as symmetries in the given matrices tend to lead to symmetries in the pseudospectra. It is hard not to see horizontal and vertical symmetry in all the images in Figures 1 and 2. These symmetries are a manifestation of the two symmetries in the underlying SSH systems, mirror symmetry and sublattice (chiral) symmetry. That this leads to symmetry with both forms of pseudospectrum is then a consequence of the following theorem.

Theorem IV.1. Suppose A_1, \ldots, A_d are Hermitian matrices. Suppose S is a unitary matrix such that $SA_j = A_jS$ for all j except that $SA_d = -A_dS$. Then

$$\mu_{\lambda}^{C}(A_1,\ldots,A_d) = \mu_{\gamma}^{C}(A_1,\ldots,A_d)$$

This is the author's peer reviewed, accepted manuscript. However, the online version of record will be different from this version once it has been copyedited and typeset

PLEASE CITE THIS ARTICLE AS DOI: 10.1063/5.009833

and

$$\mu_{\lambda}^{Q}(A_1,\ldots,A_d) = \mu_{\gamma}^{Q}(A_1,\ldots,A_d)$$

for
$$\gamma = (\lambda_1, \lambda_2, \dots, \lambda_{d-1}, -\lambda_d)$$
.

Proof. Since

$$S(A_d - \lambda_d)^2 S^{\dagger} = (-A_d - \lambda_d)^2 = (A_d + \lambda_d)^2$$

and

$$S(A_i - \lambda_i)^2 S^{\dagger} = (A_i - \lambda_i)^2$$

for the other j we find that

$$SQ_{\lambda}(A_1,\ldots,A_d)S^{\dagger} = Q_{\gamma}(A_1,\ldots,A_d).$$

These two composite matrices are unitarily equivalent, so they have the same eigenvalues.

For the localizer, we first fix some choice of the Γ_j . Notice that $\Gamma_1, \Gamma_2, \dots, \Gamma_{d-1}, -\Gamma_d$ is also a representation of the generators of the appropriate Clifford algebra. When d is even the complex Clifford algebra is isomorphic to $\mathbf{M}_{2^d(\mathbb{C})}$ which means that these two representations are unitarily equivalent. Indeed, the unitary matrix $R = \Gamma_1 \Gamma_2 \cdots \Gamma_{d-1}$ satisfies $R\Gamma_d R^{\dagger} = -\Gamma_d$ and $R\Gamma_j R^{\dagger} = \Gamma_j$ for all other j. We now find

$$(S \otimes R) \left((A_d - \lambda_d) \otimes \Gamma_d \right) \left(S \otimes R \right)^{\dagger} = \left(-A_d - \lambda_d \right) \otimes \left(-\Gamma_d \right) = \left(A_d + \lambda_d \right) \otimes \Gamma_d$$

and, for the other j,

$$(S \otimes R) ((A_j - \lambda_j) \otimes \Gamma_j) (S \otimes R)^{\dagger} = (A_j - \lambda_j) \otimes \Gamma_j.$$

Therefore

$$(S \otimes R) L_{\lambda}(A_1, \ldots, A_d) (S \otimes R)^{\dagger} = L_{\gamma}(A_1, \ldots, A_d)$$

and this tells us that the spectra of the two localizers are equal.

When d is odd, $\Gamma_1, \Gamma_2, \dots, \Gamma_{d-1}, -\Gamma_d$ is no longer equivalent to the original choice of matrices. However, we can still utilize R which now gives us $R\Gamma_d R^{\dagger} = \Gamma_d$ and $R\Gamma_j R^{\dagger} = -\Gamma_j$ for all other j. Therefore

$$(S \otimes R) L_{\lambda}(A_1, \dots, A_d) (S \otimes R)^{\dagger} = -L_{\gamma}(A_1, \dots, A_d)$$

which is good enough, as we are only interested in the absolute values of the eigenvalues.

V. WHERE IS THE K-THEORY?

For all its advantages, the quadratic pseudospectrum seems to not see K-theory. There are many forms of K-theory, the one most relevant here being the K-theory of C^* -algebras, real or complex [45, 52]. Given a C^* -algebra \mathcal{A} , for example the algebra of real or the algebra of complex n-by-n matrices, the various K-theory groups of \mathcal{A} can be defined in terms of homotopy classes of some structured class of matrices over \mathcal{A} . Since matrices of matrices are essentially just matrices, it is reasonable here to think of homotopy classes within some subclass of matrices.

In the case of complex matrices, one can define K_0 by looking at Hermitian invertible matrices. The more standard picture is to look at Hermitian projections, but all that is really needed is keeping a spectral gap around some fixed point. We prefer that fixed point to be zero. Then we note that a path of invertible matrices cannot move an eigenvalue from positive to negative. Indeed, $K_0(\mathbf{M}_n(\mathbb{C}))$ is isomorphic to \mathbb{Z} , and one can determine which element in \mathbb{Z} is represented by an invertible Hermitian matrix by looking at the number of positive eigenvalues it has minus the number of negative eigenvalues (i.e. its signature).

In the case of real matrices, we can define K_0 just as in the complex case, and we can define K_1 by looking at all invertible matrices. We know two real invertible matrices of the same size can be connected by a path of invertible matrices if and only if their determinant has the same sign. Once all the formalism is sorted out, one finds this basic fact

PLEASE CITE THIS ARTICLE AS DOI: 10.1063/5.0098336

leads to the isomorphism $K_1(\mathbf{M}_n(\mathbb{R})) \cong \mathbb{Z}_2$. The group $K_2(\mathbf{M}_n(\mathbb{R}))$ is a bit more exotic, being related to the Pfaffian rather than the determinant. For details, see [6].

To get a sense of why the quadratic composite operator seems to be unable to detect K-theory, we consider the straight path of systems with H_t as in (I.2) except now with

$$v = 0.7(1 - t) + 1.4t$$

and

$$w = 1.4(1-t) + 0.7t.$$

We fix $\lambda = (4,0)$ so we are looking at zero energy and at the approximate middle in position. (Staying way from the exact middle eliminates a mirror symmetry that confuses things.) Instead of just looking at the smallest singular value of $L_{(4,0)}(X,H_t)$ and $Q_{(4,0)}(X,H_t)$ we look at the entire spectrum of this composite operators. For easier comparison, we actually will plot the square root of the (positive) eigenvalues of the quadratic composite operator.

Since $[H_t, X]$ is not zero, and indeed has no null space, there can be no common eivenvectors for H_t and X. Thus the quadratic pseudospectrum of (X, H_t) is never zero, and so Proposition II.1, tells us that quadratic composite operator is never singular. Thus we are looking at a path of invertible matrices and we cannot use it to detect a change of any topological index. See Figure 6-a.

The spectrum of the localizer, shown in Figure 6-b, is more promising. However, the upward and downward moving eigenvalues appear as if they should somehow cancel out. We explain below that there is a symmetry here in the localizer when d=2 which is forcing the entire spectrum of the localizer to be symmetric about zero.

Let

$$\Gamma = \begin{bmatrix} 1 & & & & & \\ & -1 & & & & \\ & & 1 & & & \\ & & & -1 & & \\ & & & & 1 & \\ & & & & -1 & \\ & & & & & 1 \\ & & & & & -1 \end{bmatrix}$$

be the grading operator for which we have $H_t\Gamma = -\Gamma H_t$ and $X\Gamma = \Gamma X$, reflecting the chiral nature of this system. Let $\ddot{X} = X - 4I$. We find

$$L_{(0,4)}(X, H_t) = \begin{bmatrix} 0 & \tilde{X} - iH_t \\ \tilde{X} + iH_t & 0 \end{bmatrix} = \begin{bmatrix} \Gamma \\ I \end{bmatrix} \begin{bmatrix} 0 & \left(\left(\tilde{X} + iH_t \right) \Gamma \right)^{\dagger} \\ \left(\tilde{X} + iH_t \right) \Gamma & 0 \end{bmatrix} \begin{bmatrix} \Gamma \\ I \end{bmatrix}^{\dagger}$$

which tells us that

$$\alpha \in \sigma\left(L_{(0,4)}(X, H_t)\right) \iff \pm \alpha \in \sigma\left(\left(\tilde{X} + iH_t\right)\Gamma\right).$$

Notice we are using σ_x and σ_y as the default choice of Γ matrices, for reasons we explain in Sec. IV. Also, we are using perhaps the less-common convention in the concrete interpretation of a tensor of matrices.

We plot the spectrum of this "reduced localizer" in Figure 6-c. The details of how this spectral imbalance is a proper K-theory invariant can be found in [32]. We mention it here to explain that the positive semidefinite nature of the quadratic composite operator makes it immune to K-theory.

In other symmetry classes, the correct index is found using the sign of the determinant of a matrix that has real elements. Notice here that $(\tilde{X} + iH_t)\Gamma$ has real determinant and an odd number of eigenvalues passing from positive to negative would have been reflected in the sign of the determinant. We will look at another small example in the next section that corresponds to a symmetry class where the expected index is \mathbb{Z}_2 index that can be found using the sign of a determinant of a similar matrix. The details of why this index is a reasonable index are more complicated [16]. Again, the fact that the quadratic composite operator is positive means its determinant is stuck being positive, so cannot detect this sort of invariant either.

ACCEPTED MANUSCRIPT

is the author's peer reviewed, accepted manuscript. However, the online version of record will be different from this version once it has been copyedited and typeset

PLEASE CITE THIS ARTICLE AS DOI: 10.1063/5.0098336

Manicillatica

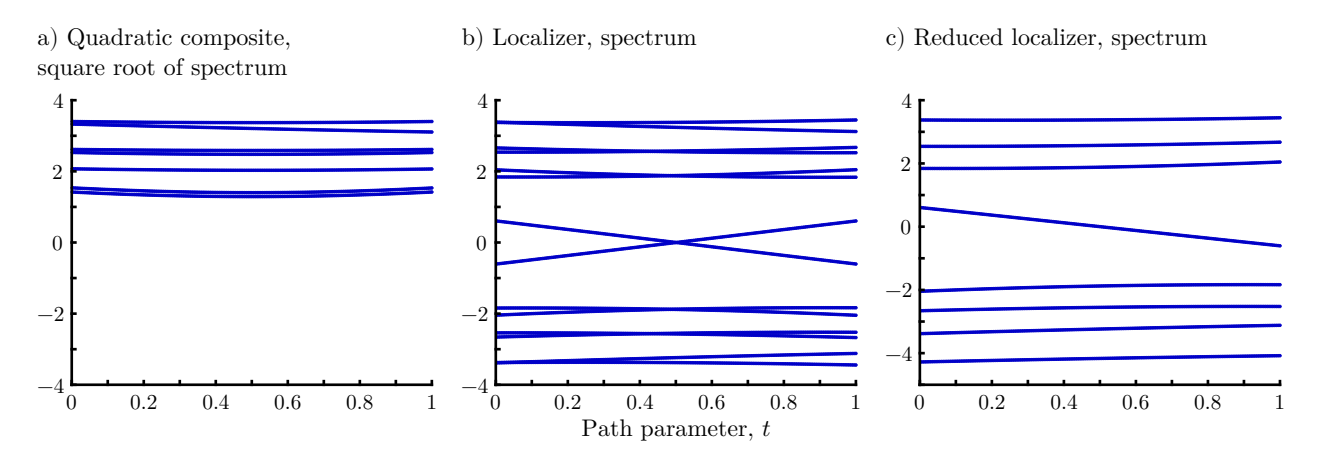


FIG. 6. We work along a path from a trivial system at t=0 to a topological system at t=1. In (a) we look at the full spectrum of the quadratic composite operator, fixing $\lambda = (4,0)$. In (b) we show the spectrum of the localizer. In (c) we show the spectrum of the reduced localizer, $((X-4)+iH_t)\Gamma$.

VI. EDGE AND BULK STATES

Next we look at examples of the quadratic spectrum for matrices that represent observables in a physically interesting system. Although our analysis begins with a general two-dimensional lattice, we will later specialize to a specific model that consists of half of the low-energy tight-binding model for HgTe [22, 23, 42], where the two spin sectors are decoupled.

In a general 2D lattice, there are three observables, the Hamiltonian H and matrices X and Y representing position. We make the specific choice for the Γ matrices for the Clifford representation to be the Pauli spin matrices. Now the localizer takes the form

$$L_{(x,y,E)}(X,Y,H) = (X-x) \otimes \sigma_x + (Y-y) \otimes \sigma_y + (H-E) \otimes \sigma_z$$
$$= \begin{bmatrix} H-E & X-iY-(x-iy) \\ X+iY-(x+iy) & -H+E \end{bmatrix}.$$

We also can assume that X and Y commute, so (II.4) becomes

$$(L_{(x,y,E)}(X,Y,H))^2 = Q_{(x,y,E)}(X,Y,H) \otimes I + \begin{bmatrix} 0 & [H,X+iY] \\ ([H,X+iY])^{\dagger} & 0 \end{bmatrix}$$
 (VI.1)

and (II.3) becomes

$$\left| \left(\mu_{\pmb{\lambda}}^Q(X,Y,H) \right)^2 - \left(\mu_{\pmb{\lambda}}^C(X,Y,H) \right)^2 \right| \le \left\| [H,X+iY] \right\|. \tag{VI.2}$$

The units for H and for X and Y are not necessarily compatible, so we must introduce a constant κ that represents changing units for measuring position. Mathematically this just means we compute joint pseudospectra of $(\kappa X, \kappa Y, H)$. If κ is too close to zero the pseudospectra will only really see the system's energy spectrum. If κ is too large the pseudospectra will only really see position information.

We illustrate the quadratic and Clifford pseudospectra using the Qi-Wu-Zhang (QWZ) model, a standard model of a Chern insulator [42]. The real-space tight-binding model for this lattice consists of a square lattice with a copy of \mathbb{C}^2 at each site, i.e., a system with two orbitals per lattice site. That is, our Hilbert space is $\ell^2(\mathbb{Z}^2) \otimes \mathbb{C}^2$. Thus, our default lattice constant is 1 so working with κX and κY resets the lattice constant to κ in units of the Hamiltonian (in this case, energy). The QWZ tight-binding Hamiltonian is

$$H = -2t \sum_{m_x} \sum_{m_y} \left(|m_x + 1, m_y\rangle \langle m_x, m_y| \otimes \frac{\sigma_z + i\sigma_x}{2} + h.c. \right)$$
$$-2t \sum_{m_x} \sum_{m_y} \left(|m_x, m_y + 1\rangle \langle m_x, m_y| \otimes \frac{\sigma_z + i\sigma_y}{2} + h.c. \right) + 2t \sum_{m_x} \sum_{m_y} |m_x, m_y\rangle \langle m_x, m_y| \otimes \sigma_z, \quad (VI.3)$$

PLEASE CITE THIS ARTICLE AS DOI: 10.1063/5.0098336

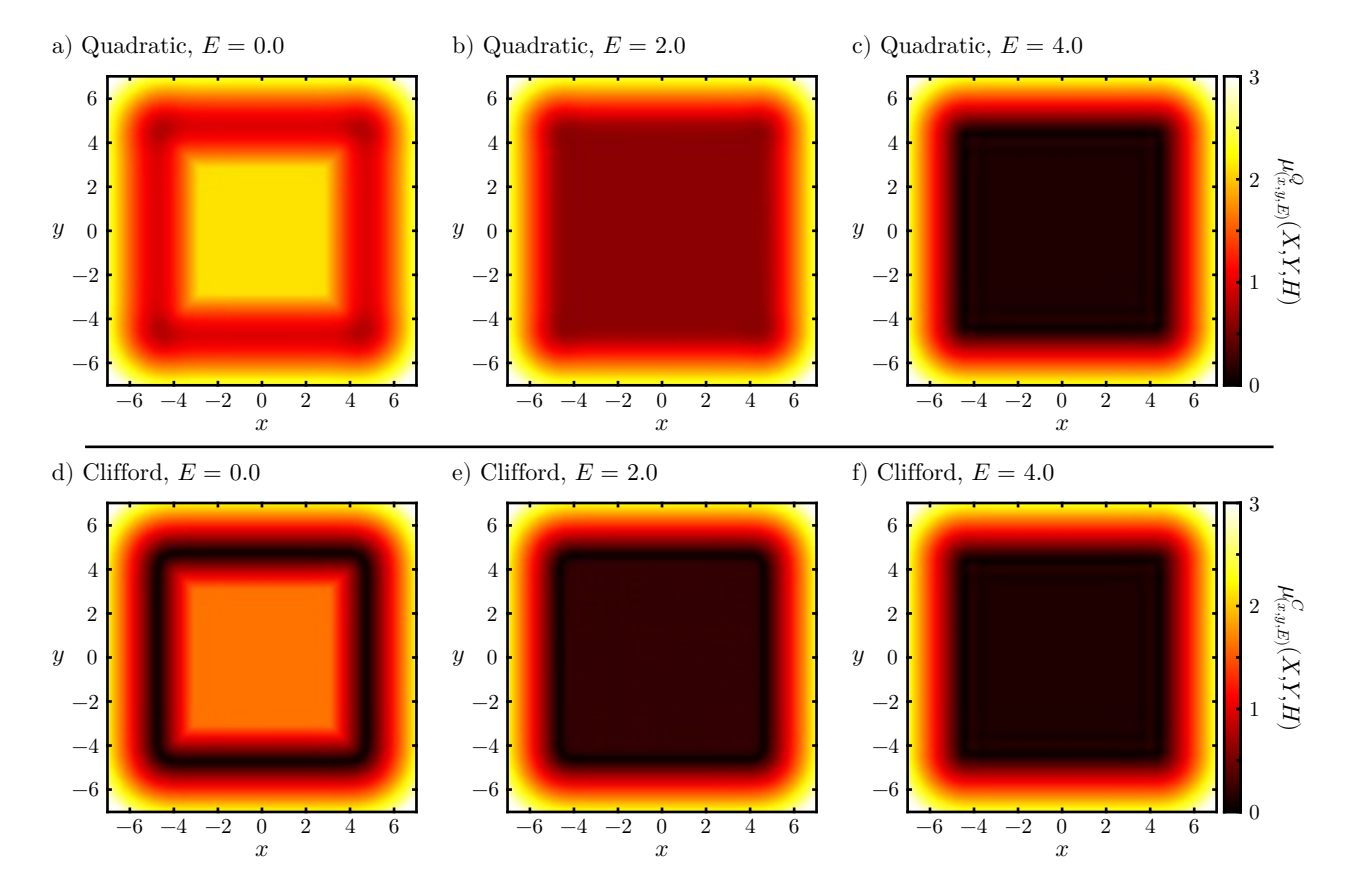


FIG. 7. Here we look at slices of both flavors of pseudospectra for a very standard Chern insulator model. This is the same model as used in [29, 31] and is here on 20-by-20 lattice. The lattice unit here is set to 0.5 so the model has x and y coordinates in the range -5 to 5. The spectral gap in the bulk Hamiltonian is roughly between -1 and 1.

where t=1 is the coefficient that sets the scale for the couplings and $|m_x, m_y\rangle$ indexes the lattice site at m_x, m_y . Given the ratio of the on-site energy to the couplings, this particular QWZ lattice is in a non-trivial topological phase with Chern number C=-1 [2], and this choice of parameters is chosen to match with the study involving the Bott index in [31]. This lattice's bulk spectrum is the two intervals between ± 1 and ± 6 .

We impose open boundary conditions and first look at a small system, just 20-by-20 sites. Since $||[H, X + iY]|| \approx 2.79$ we expect that unless we set κ to be well less than 1 there will be significant differences between the two pseudospectra. We also do not want $\kappa \approx 0$ since that would cause both pseudospectra to just reflect the system's energy spectrum. In Figure 7 we use $\kappa = 0.5$. The Clifford pseudospectrum goes to zero near the boundary when at zero energy; this is expected, as it is only when an eigenvalue of the localizer crosses zero that we can see a change in index [29]. The quadratic pseudospectrum stays relatively large, but still bounded by Eq. (VI.2).

Looking at smaller κ will tell us more about edge states that are really localized in energy. However, we need to look to a larger system to avoid the bulk blending into the edges. In Figure 8 we use $\kappa = 0.05$ while examining a 100-by-100 lattice. The two pseudospectra are now much closer to each other.

For every choice of x, y and κ that leads to small value of $\mu_{(x,y,0)}^Q(\kappa X,\kappa Y,H)$ there is an associated unit vector v. This can be easily computed as an eigenvector of $Q_{\lambda}(\kappa X,\kappa Y,H)$ or as a right singular vector of

$$\begin{bmatrix} \kappa(X-x) \\ \kappa(Y-y) \\ H-E \end{bmatrix}$$

as in Prop. II.1. Figure 9 shows the nature of this state for (x, y, E) = (49, 0, 0), which represents a point in the middle of the bottom of the lattice, slightly in from the edge. The system is centered at 0 and extends in both directions from -49.5 to +49.5. This state is computed for various values of κ . As expected, smaller κ results in better localization in energy and more dispersion in position.



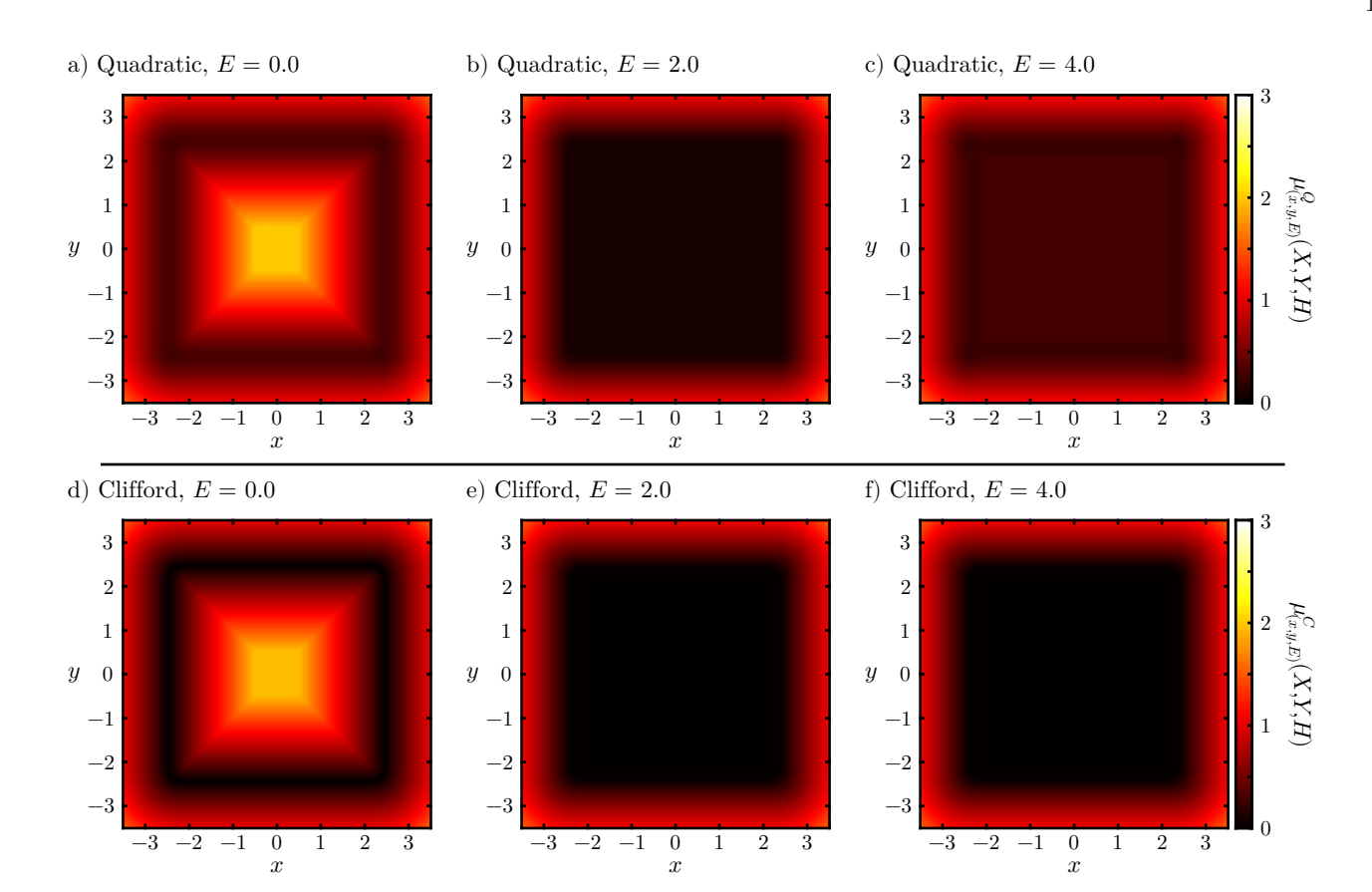


FIG. 8. Here we look at slices of both flavors of pseudospectra for a very standard Chern insulator model. This is the same model as used in [29, 31] and is here on 100-by-100 lattice. The lattice unit here is set to 0.05 so the model has x and y coordinates in the range -2.5 to 2.5.

Pseudospectral techniques hold promise in the study of topological photonic systems since they can detect K-theory even when a complete band gap does not exist [10]. For example, one can look at a photonic Chern metal, as in [11].

A. Boundary states degenerate with the bulk spectrum

The quadratic pseudospectrum can also be used to identify localized states (or localized quasi-modes with finite lifetimes) amidst the background of a degenerate bulk spectrum. To demonstrate this feature, we use a model of a higher-order topological metal that can exhibit localized corner states despite these states being within the spectral extent of the system's bulk bands [4, 9, 10]. This lattice's real-space tight-binding description consists of a square lattice with four sites within each unit cell,

$$\begin{split} H = -t_{\text{in}} \sum_{m_x, m_y} (|m_x, m_y, 2\rangle \langle m_x, m_y, 1| + |m_x, m_y, 3\rangle \langle m_x, m_y, 2| + \\ + |m_x, m_y, 4\rangle \langle m_x, m_y, 3| + |m_x, m_y, 1\rangle \langle m_x, m_y, 4| + h.c.) \\ -t_{\text{out}} \sum_{m_x, m_y} (|m_x - 1, m_y, 2\rangle \langle m_x, m_y, 1| + |m_x, m_y - 1, 4\rangle \langle m_x, m_y, 1| + \\ + |m_x, m_y - 1, 3\rangle \langle m_x, m_y, 2| + |m_x - 1, m_y, 3\rangle \langle m_x, m_y, 4| + h.c.) \,, \quad \text{(VI.4)} \end{split}$$

that are coupled together so as to obey chiral symmetry. Here, $t_{\rm in}$ and $t_{\rm out}$ are the within and between unit cell coupling strengths, respectively, while the final index, α in the states $|m_x, m_y, \alpha\rangle$ denotes the specific site within each unit cell.

Previously, the higher-order topological metal lattice has been shown to exhibit topological corner-localized states at E = 0 that are robust to system perturbations, even in the absence of a bulk band gap at E = 0 [10], see also Fig. 10a-c.

PLEASE CITE THIS ARTICLE AS DOI; 10.1063/5.0098336



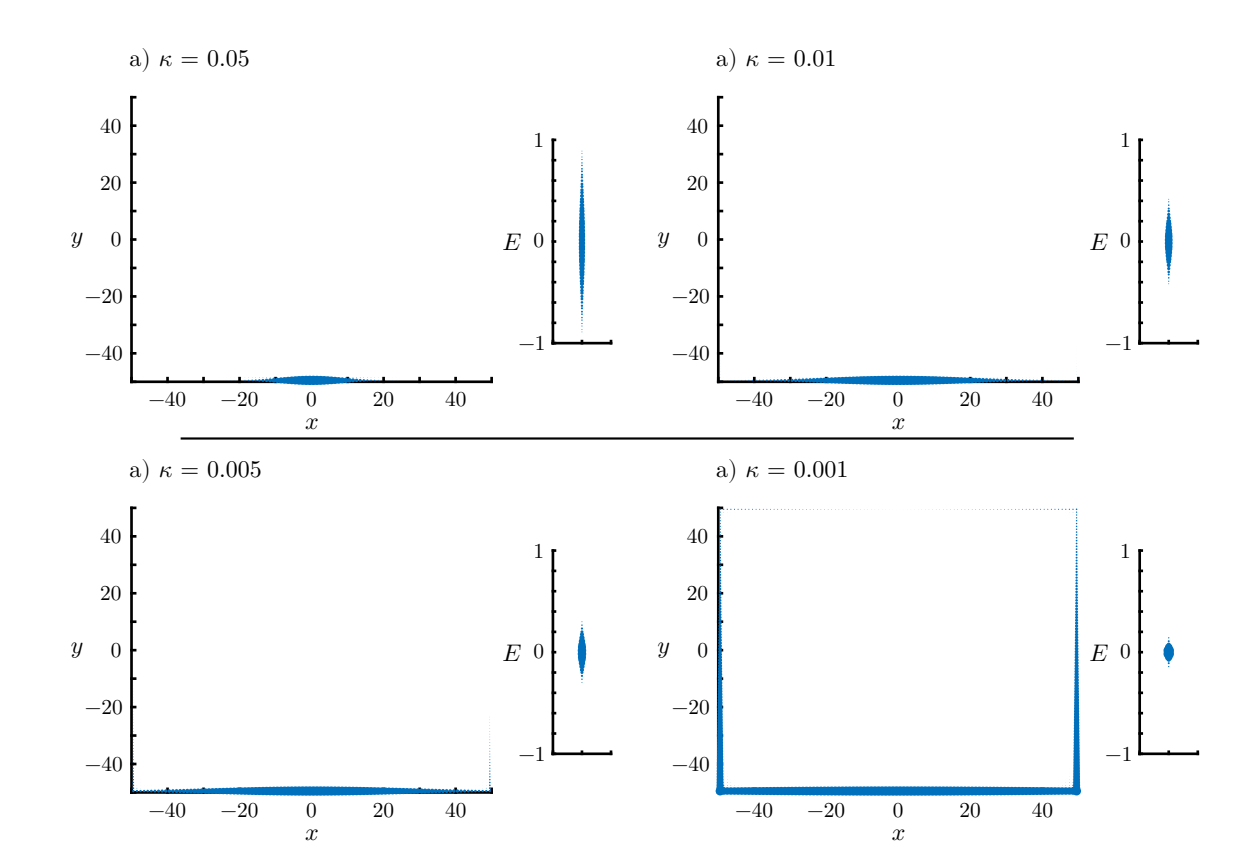


FIG. 9. Edge states for a Chern insulator found with different values of κ in the Quadratic pseudospectra. Each panel shows the distribution (large plot) in space and the distribution in energy (small plat) for a state selected as an eigenvalue of $Q_{\lambda}(\kappa X, \kappa Y, H)$ for a fixed value of $\lambda = (x, y, E) = (49, 0, 0)$ as κ varies.

Here, we instead focus on how the quadratic pseudospectrum can identify the corner-localized states, Fig. 10d-f, despite the degenerate background. In particular, by choosing λ to be at one of the lattice's corners and at E=0, the eigenstate corresponding to the smallest eigenvalue of $Q_{\lambda}(X,Y,H)$ very closely resembles a corner eigenstate that can be found in the lattice's degenerate subspace at E=0, see Fig. 10e. In contrast, choosing λ to be at the lattice's center (and still at E=0) yields an eigenstate of $Q_{\lambda}(X,Y,H)$ that is a superposition of bulk modes (eigenstates of H) localized near λ in both position and energy, see Fig. 10f.

VII. CONCLUSION

In conclusion, we have established the necessary definitions and theorems for both understanding the utility of the quadratic composite operator and quadratic pseudospectrum in physical systems, as well as the relationship between the quadratic and Clifford pseudospectra. Moreover, we have proven that the quadratic pseudospectrum is local, which has two important consequences. First, the numerical difficultly in calculating the quadratic pseudospectrum plateaus beyond a certain system size, where the error in the calculation incurred through the truncation becomes negligible. Second, this provides us a new tool to related bound states in a large system to bound states in a more easily understood truncated system. This was already possible using the truncation bound known for the localizer in [30], but the bounds in Sect. III are simpler.

On a more fundamental level, the quadratic composite operator and pseudospectrum represent the most straightforward method for approaching systems with incompatible observables, as it both minimizes the eigen-error in the joint approximate spectrum and does not increase the computational complexity of the system. If the system is suspected of possessing non-trivial K-theory, this can then be calculated using the localizer where the quadratic gap is maximized, which will typically coincide with large localizer gaps due to Prop. II.4. Similarly, any topological boundary-localized states that exist in systems with non-trivial K-theory in their bulk can also be found near minima in the system's



PLEASE CITE THIS ARTICLE AS DOI: 10.1063/5.0098336

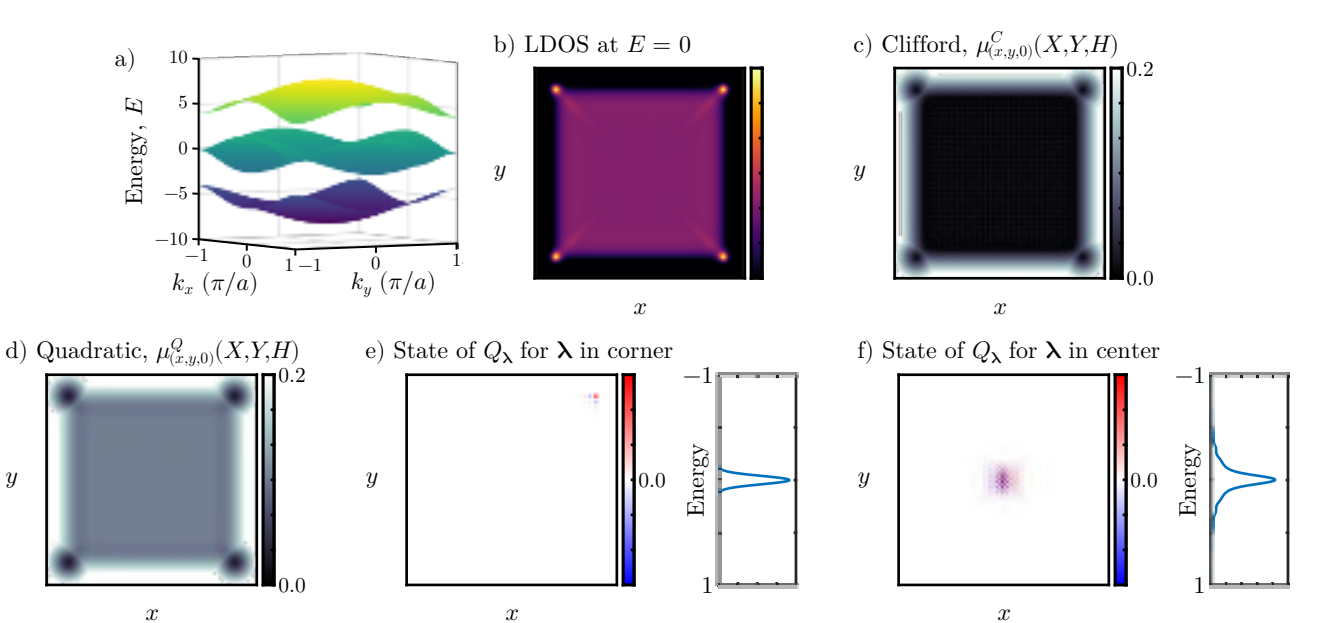


FIG. 10. (a) Bulk band structure for a higher-order topological metal with $t_{\rm in}=1$ and $t_{\rm out}=3$. (b) Local density of states at E=0 for a finite higher-order topological metal with 30-by-30 unit cells. (c) Clifford pseudospectrum for this system at E=0 and $\kappa=0.1$. (d) Quadratic pseudospectrum for this system at E=0 and $\kappa=0.1$. (e) (left) Spatial distribution of the real part of the eigenstate of $Q_{\lambda}(\kappa X, \kappa Y, H)$ corresponding to its minimal singular value, for λ chosen to be in the system's upper right corner and at E=0. (right) Distribution in energy of the eigenstate. (f) Similar to (e), except for λ chosen to be in the system's center.

quadratic gap. In particular, this may be especially relevant for studying systems whose topology is not yet known to be connected to another pseudospectra, such as non-Hermitian systems that are known to possess non-trivial topology both theoretically [5, 12, 18, 26–28, 47, 54, 56] and experimentally [8, 25, 53, 58].

ACKNOWLEDGEMENTS

T.L. acknowledges support from the National Science Foundation, grant DMS-2110398. A.C. and T.L. acknowledge support from the Center for Integrated Nanotechnologies, an Office of Science User Facility operated for the U.S. Department of Energy (DOE) Office of Science, and the Laboratory Directed Research and Development program at Sandia National Laboratories. Sandia National Laboratories is a multimission laboratory managed and operated by National Technology & Engineering Solutions of Sandia, LLC, a wholly owned subsidiary of Honeywell International, Inc., for the U.S. DOE's National Nuclear Security Administration under contract DE-NA-0003525. The views expressed in the article do not necessarily represent the views of the U.S. DOE or the United States Government. F. V. acknowledges support from the Scientific Computing Innovation Center of UNAH, under project PI-063-DICIHT.

^[1] Alexander Altland and Martin R. Zirnbauer. Nonstandard symmetry classes in mesoscopic normal-superconducting hybrid structures. *Phys. Rev. B*, 55(2):1142–1161, January 1997.

^[2] János K Asbóth, László Oroszlány, and András Pályi. A short course on topological insulators. Lecture notes in physics, 919:166, 2016.

^[3] A. Bansil, Hsin Lin, and Tanmoy Das. Colloquium: Topological band theory. Rev. Mod. Phys., 88(2):021004, June 2016. Publisher: American Physical Society.

^[4] Wladimir A. Benalcazar and Alexander Cerjan. Bound states in the continuum of higher-order topological insulators. *Phys. Rev. B*, 101:161116, Apr 2020.

^[5] Emil J. Bergholtz, Jan Carl Budich, and Flore K. Kunst. Exceptional topology of non-Hermitian systems. Rev. Mod. Phys., 93(1):015005, February 2021. Publisher: American Physical Society.

the online version of record will be different from this version once it has been copyedited and typeset

PLEASE CITE THIS ARTICLE AS DOI: 10.1063/5.0098336

accepted manuscript. However,

- [6] Jeffrey L. Boersema and Terry A. Loring. K-theory for real C^* -algebras via unitary elements with symmetries. New York J. Math., 22:1139–1220, 2016.
- [7] J.F. Cardoso and A. Souloumiac. Jacobi angles for simultaneous diagonalization. SIAM Journal on Matrix Analysis and Applications, 17(1):161–164, 1996.
- [8] Alexander Cerjan, Sheng Huang, Mohan Wang, Kevin P. Chen, Yidong Chong, and Mikael C. Rechtsman. Experimental realization of a Weyl exceptional ring. *Nat. Photonics*, 13(9):623–628, September 2019.
- [9] Alexander Cerjan, Marius Jürgensen, Wladimir A. Benalcazar, Sebabrata Mukherjee, and Mikael C. Rechtsman. Observation of a higher-order topological bound state in the continuum. *Phys. Rev. Lett.*, 125:213901, Nov 2020.
- [10] Alexander Cerjan and Terry A Loring. Local invariants identify topology in metals and gapless systems. *Physical Review B*, 106(6):064109, 2022.
- [11] Alexander Cerjan and Terry A. Loring. An operator-based approach to topological photonics. *Nanophotonics*, 11(21), 4765–4780, 2022.
- [12] Alexander Cerjan, Meng Xiao, Luqi Yuan, and Shanhui Fan. Effects of non-Hermitian perturbations on Weyl Hamiltonians with arbitrary topological charges. *Phys. Rev. B*, 97(7):075128, February 2018.
- [13] Bin Chen and Shao-Ming Fei. Sum uncertainty relations for arbitrary n incompatible observables. Scientific reports, 5(1):1–6, 2015.
- [14] Ching-Kai Chiu, Jeffrey C. Y. Teo, Andreas P. Schnyder, and Shinsei Ryu. Classification of topological quantum matter with symmetries. *Rev. Mod. Phys.*, 88(3):035005, August 2016. Publisher: American Physical Society.
- [15] Patrick Debonis, Terry Loring, and Roman Sverdlov. Surfaces and hypersurfaces as the joint spectrum of matrices. *Rocky Mountain J. Math.*, 52(4):1319–1343, 2022.
- [16] Nora Doll and Hermann Schulz-Baldes. Skew localizer and \mathbb{Z}_2 -flows for real index pairings. Adv. Math., 392:Paper No. 108038, 42, 2021.
- [17] Gene H. Golub and Charles F. Van Loan. *Matrix computations*. Johns Hopkins Studies in the Mathematical Sciences. Johns Hopkins University Press, Baltimore, MD, third edition, 1996.
- [18] Zongping Gong, Yuto Ashida, Kohei Kawabata, Kazuaki Takasan, Sho Higashikawa, and Masahito Ueda. Topological Phases of Non-Hermitian Systems. *Phys. Rev. X*, 8(3):031079, September 2018.
- [19] Walter A. Harrison. Solid State Theory. Courier Corporation, January 1980.
- [20] M. Z. Hasan and C. L. Kane. Colloquium: Topological insulators. Rev. Mod. Phys., 82(4):3045–3067, November 2010.
- [21] I. Komis, D. Kaltsas, S. Xia, H. Buljan, Z. Chen, and K. G. Makris. Robustness versus sensitivity in non-Hermitian topological lattices probed by pseudospectra. *Physical Review Research*, 4(4):043219, 2022.
- [22] Markus König, Hartmut Buhmann, Laurens W. Molenkamp, Taylor Hughes, Chao-Xing Liu, Xiao-Liang Qi, and Shou-Cheng Zhang. The Quantum Spin Hall Effect: Theory and Experiment. J. Phys. Soc. Jpn., 77:031007, March 2008. Publisher: The Physical Society of Japan.
- [23] Markus König, Steffen Wiedmann, Christoph Brüne, Andreas Roth, Hartmut Buhmann, Laurens W. Molenkamp, Xiao-Liang Qi, and Shou-Cheng Zhang. Quantum Spin Hall Insulator State in HgTe Quantum Wells. *Science*, 318(5851):766–770, November 2007.
- [24] D Krejčiřík, Petr Siegl, Milos Tater, and Joe Viola. Pseudospectra in non-hermitian quantum mechanics. *Journal of mathematical physics*, 56(10):103513, 2015.
- [25] Mark Kremer, Tobias Biesenthal, Lukas J. Maczewsky, Matthias Heinrich, Ronny Thomale, and Alexander Szameit. Demonstration of a two-dimensional \mathcal{PT} -symmetric crystal. Nat. Commun., 10(1):435, January 2019.
- [26] Flore K. Kunst, Elisabet Edvardsson, Jan Carl Budich, and Emil J. Bergholtz. Biorthogonal Bulk-Boundary Correspondence in Non-Hermitian Systems. *Phys. Rev. Lett.*, 121(2):026808, July 2018.
- [27] Tony E. Lee. Anomalous Edge State in a Non-Hermitian Lattice. Phys. Rev. Lett., 116(13):133903, April 2016.
- [28] Daniel Leykam, Konstantin Y. Bliokh, Chunli Huang, Y. D. Chong, and Franco Nori. Edge Modes, Degeneracies, and Topological Numbers in Non-Hermitian Systems. *Phys. Rev. Lett.*, 118(4):040401, January 2017.
- [29] Terry A. Loring. K-theory and pseudospectra for topological insulators. Ann. Physics, 356:383–416, 2015.
- [30] Terry A. Loring. A guide to the Bott index and localizer index. arXiv:1907.11791, 2019.
- [31] Terry A. Loring and Matthew B. Hastings. Disordered topological insulators via C*-algebras. Europhys. Lett. EPL, 92:67004, 2010.
- [32] Terry A. Loring and Hermann Schulz-Baldes. Finite volume calculation of K-theory invariants. New York J. Math., 23:1111–1140, 2017.
- [33] Terry A. Loring and Hermann Schulz-Baldes. The spectral localizer for even index pairings. J. Noncommut. Geom., 14(1):1–23, 2020
- [34] Terry A. Loring and Fredy Vides. Computing truncated joint approximate eigenbases for model order reduction. In *Discussion Contributions 10th Vienna Conference on Mathematical Modelling*, volume 17. ARGESIM, 2022. https://doi.org/10.11128/arep.17.a17209.
- [35] Lorenzo Maccone and Arun K Pati. Stronger uncertainty relations for all incompatible observables. *Physical review letters*, 113(26):260401, 2014.
- [36] KG Makris. Transient growth and dissipative exceptional points. Physical Review E, 104(5):054218, 2021.
- [37] Nicola Marzari, Arash A. Mostofi, Jonathan R. Yates, Ivo Souza, and David Vanderbilt. Maximally localized wannier functions: Theory and applications. Rev. Mod. Phys., 84:1419–1475, Oct 2012.

ACCEPTED MANUSCRIPT

PLEASE CITE THIS ARTICLE AS DOI: 10.1063/5.0098336

the online version of record will be different from this version once it has been copyedited and typeset

- [38] Eric J Meier, Fangzhao Alex An, and Bryce Gadway. Observation of the topological soliton state in the Su–Schrieffer–Heeger model. *Nature communications*, 7(1):1–6, 2016.
- [39] Jonathan Michala, Alexander Pierson, Terry A. Loring, and Alexander B. Watson. Wave-packet propagation in a finite topological insulator and the spectral localizer index. *Involve*, 14(2):209–239, 2021.
- [40] Nobuyuki Okuma and Masatoshi Sato. Hermitian zero modes protected by nonnormality: Application of pseudospectra. *Physical Review B*, 102(1):014203, 2020.
- [41] Tomoki Ozawa, Hannah M. Price, Alberto Amo, Nathan Goldman, Mohammad Hafezi, Ling Lu, Mikael C. Rechtsman, David Schuster, Jonathan Simon, Oded Zilberberg, and Iacopo Carusotto. Topological photonics. Rev. Mod. Phys., 91(1):015006, March 2019.
- [42] Xiao-Liang Qi, Yong-Shi Wu, and Shou-Cheng Zhang. Topological quantization of the spin Hall effect in two-dimensional paramagnetic semiconductors. *Phys. Rev. B*, 74(8):085308, August 2006. Publisher: American Physical Society.
- [43] Shinsei Ryu, Andreas P. Schnyder, Akira Furusaki, and Andreas W. W. Ludwig. Topological insulators and superconductors: tenfold way and dimensional hierarchy. New J. Phys., 12(6):065010, June 2010.
- [44] Lukas Schneiderbauer and Harold C Steinacker. Measuring finite quantum geometries via quasi-coherent states. *Journal of Physics A: Mathematical and Theoretical*, 49(28):285301, 2016.
- [45] Herbert Schröder and Herbert Schröder. K-theory for real C*-algebras and applications. Longman Scientific & Technical Harlow, 1993.
- [46] Hermann Schulz-Baldes and Tom Stoiber. Spectral localization for semimetals and Callias operators. arXiv:2203.15014 [math-ph], March 2022. arXiv:2203.15014.
- [47] Huitao Shen, Bo Zhen, and Liang Fu. Topological Band Theory for Non-Hermitian Hamiltonians. *Phys. Rev. Lett.*, 120(14):146402, April 2018.
- [48] A Sivan and M Orenstein. Multiple crossed non-Hermitian Su-Schrieffer-Heeger chains coupled via a mutual defect site. arXiv preprint arXiv:2202.07655, 2022.
- [49] W. P. Su, J. R. Schrieffer, and A. J. Heeger. Solitons in polyacetylene. Physical review letters, 42(25):1698, 1979.
- [50] L. N. Trefethen. Pseudospectra of matrices. In Numerical analysis 1991 (Dundee, 1991), volume 260 of Pitman Res. Notes Math. Ser., pages 234–266. Longman Sci. Tech., Harlow, 1992.
- [51] Lloyd N. Trefethen and Mark Embree. Spectra and pseudospectra. Princeton University Press, Princeton, NJ, 2005. The behavior of nonnormal matrices and operators.
- [52] N. E. Wegge-Olsen. K-theory and C^* -algebras. Oxford Science Publications. The Clarendon Press, Oxford University Press, New York, 1993. A friendly approach.
- [53] S. Weimann, M. Kremer, Y. Plotnik, Y. Lumer, S. Nolte, K. G. Makris, M. Segev, M. C. Rechtsman, and A. Szameit. Topologically protected bound states in photonic parity-time-symmetric crystals. *Nat. Mater.*, 16(4):433–438, April 2017.
- [54] Charles C. Wojcik, Xiao-Qi Sun, Tomá š Bzdušek, and Shanhui Fan. Homotopy characterization of non-Hermitian Hamiltonians. *Phys. Rev. B*, 101(20):205417, May 2020. Publisher: American Physical Society.
- [55] Di Xiao, Ming-Che Chang, and Qian Niu. Berry phase effects on electronic properties. Rev. Mod. Phys., 82(3):1959–2007, July 2010.
- [56] Shunyu Yao and Zhong Wang. Edge States and Topological Invariants of Non-Hermitian Systems. *Phys. Rev. Lett.*, 121(8):086803, August 2018.
- [57] Ken Huai-Che Yeh. Emergent spacetime in matrix models. PhD thesis, University of British Columbia (Vancouver, 2018.
- [58] Julia M. Zeuner, Mikael C. Rechtsman, Yonatan Plotnik, Yaakov Lumer, Stefan Nolte, Mark S. Rudner, Mordechai Segev, and Alexander Szameit. Observation of a Topological Transition in the Bulk of a Non-Hermitian System. *Phys. Rev. Lett.*, 115(4):040402, July 2015.

